SAND2009-6089C

Super High Frequency Width Extensional Aluminum Nitride (AlN) MEMS Resonators

K. E. Wojciechowski, R. H. Olsson III, C. D. Nordquist and M. R. Tuck
Sandia National Laboratories
Albuquerque, NM, USA

***Abstract*— Width extensional (WE) super high frequency (SHF) aluminum nitride (AlN) resonators have been fabricated using optical lithography. Solidly anchored WE resonators were shown to be superior to beam anchored resonators of the same size and it was verified that simply scaling resonator area does not improve insertion loss (IL). Resonators with an IL of -6.3 dB into 50 ohms at 4.1 GHz and -7.2 dB at 6.8 GHz have been demonstrated. This type of performance at 6.8 GHz is unprecedented for contour mode resonators and represents a 12.6 dB improvement over recently reported SHF AlN resonators.**

Keywords-Aluminum Nitride; Microresonator; RF MEMS; SHF MEMS

I. INTRODUCTION

There has been recent progress in extending AlN resonator frequencies to super high frequency (SHF) bands using electron beam lithography [1-2]. We present SHF (up to 6.8 GHz) width extensional (WE) resonators that are patterned optically. In the past contour mode resonators have been anchored using quarter wave beams to minimize anchor loss. In this work we compare the performance of solidly anchored resonators to resonators anchored with quarter wave beams. Finally, it is assumed that as resonator area is scaled its insertion loss will decrease. However, the resonator shunt capacitance and added series resistance from increased finger length (L_e) causes their IL to increase or decrease less than expected.

SHF resonators were fabricated with a simplified, 2 mask AlN process without a bottom electrode or dielectric. The simplified process yields better AlN performance and higher resonator sound velocity enabling the use of optical lithography. A 6.8 GHz device is shown in Figure 1a. The solidly anchored WE resonator has a finger pitch of $\lambda/2$ = 760 nm. The active area of this device is L_e = 200µm by W_d = 58.52 µm and the overall device length is 600µm. It was hypothesized that the acoustic wave (launched in the y-direction, Figure 1a) is well confined and has minimal propagation in x-direction. Therefore, anchoring loss should not change significantly between solidly anchored and traditional contour mode resonators anchored via narrow beams [1-4]. To test this hypothesis, WE resonators with beam anchors (Figure 1b) of the same size (L_e and W_d) were fabricated. Finally, an experimental comparison was done

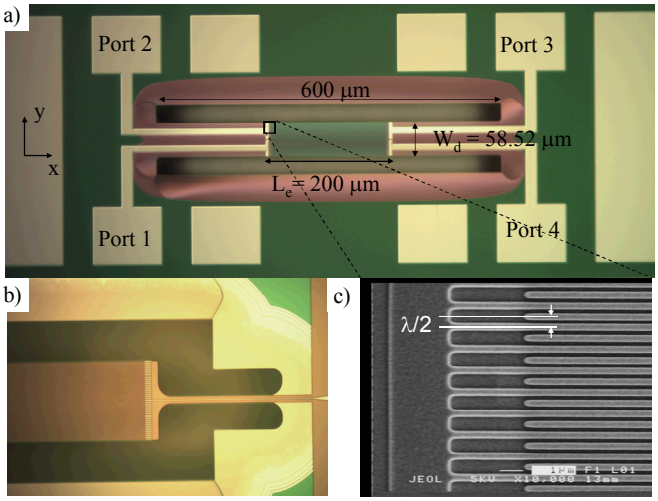

Figure 1. a) Solidly anchored width extensional four port resonator. b) Quarter wave beam anchored four port resonator. c) SEM of 250 nm line and 250 nm space ($\lambda/4$ = 500 nm) resonator fingers fabricated with optical lithography.

varying the WE resonator length (L_e), shown in Figure 1a, from 200µm to 500µm for a 4.1 GHz device. This comparison showed that increasing electrode area via L_e did very little to improve IL while increasing capacitive feed through and resistive loss. Hence increasing device area did not significantly improve IL. This was mainly due to the series resistance, R_f, of the resonator fingers since it scales with resonator length. Shunt capacitance (C_{shunt}) also plays a role however it can be resonated out with integrated inductors. These parasitics (C_{shunt}, R_f) present a significant limitation on resonator scaling.

II. SHF RESONATOR FABRICATION PROCESS

The simplified fabrication process is shown in Figure 2. It consists of the a 2 mask process similar to [1]. However in this process the lithography for the metallization is done with fine line CMOS tools. Using this simplified process yields several advantages including better film orientation and performance from direct deposition on silicon and higher resonator sound velocity by eliminating layers with relatively lower sound velocity (compared to AlN) such as the bottom electrode and insulating dielectric. The higher resonator sound velocity reduces metallization lithographic requirements (because higher material speed allows for larger electrode width and

This work was supported by the Laboratory Directed Research and Development (LDRD) program at Sandia National Laboratories. Sandia National Laboratories is a multiprogram laboratory operated by the Sandia Corporation, Lockheed Martin Company, for the United States Department of Energy's National Nuclear Security Administration under contract DE-AC04-94AL85000.

spacing (λ/4) for a given frequency). This theoretically enables the use of optical lithography to achieve resonators operating in excess of 12 GHz. Fine line CMOS lithographic tools were used to produce metallization features (metal line width and spacing) as small as 250 nm. Figure 1c shows a SEM of optically patterned electrodes for a ~ 10 GHz device with (λ/4 =250nm).

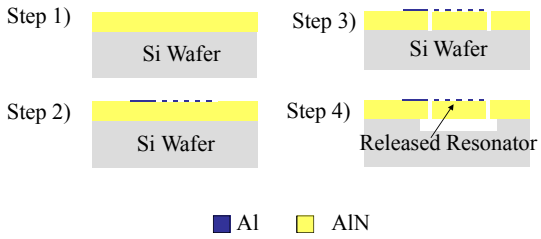

Figure 2. Simplified 2 mask SHF process. Step1) Deposit AlN, Step2) Deposit and pattern top electrode (Al). Step 3) Etch through AlN. Step 4) Release resonator.

III. SHF Resonator Design

The SHF resonator shown in Figure 1a is a solidly anchored device which is an alternative to anchoring the device with a quarter wave beam (Figure 1b). There are several advantages to this design. First it adds the freedom of using wide metal routing (not limited by beam anchor width) from the pads to the resonator. As a result this series parasitic resistance can be reduced. Second, the device is much more robust in terms of survival in high stress films. The yield of these devices was above 90% while the beam anchored had a yield of less than 10% in our process. Finally, the routing for the input and output ports do not have to be routed next to each other along a narrow beam. As a result the port-to-port feed through capacitance can be reduced when compared to a beam anchored design. For example, the average out-of-band rejection at 4 GHz for the beam anchored device was ~ 5.5 dB worse than the solidly anchored device of the same size.

A. Four Port Toplogy

Unlike previous work [1,2] this device is a four port device, and can be used in fully-differential or balun configurations. The main advantage of this topology over a two port is reduction in parasitic feed through capacitance . A typical two port resonator has a feed through capacitance in parallel with the resonator due to the finger-to-finger capacitance. At SHF the impedance of this capacitance can be comparable to the impedance of the resonator, hence severely degrading its performance and effective k_t^2. A simplified model of a two port resonator is shown in Figure 3a. In this case the finger to finger capacitance is C12. In the four port implementation the finger to finger capacitances, C14 and C23 become shunt capacitances (Figure 3b) and are one half the size of C12. The maximum feed through capacitance is from port 3 to 4, which is a single finger to finger capacitance. Hence the feed through has been reduced by a factor equal to the number of fingers. For the 4.1 GHz device this is a factor of 47.

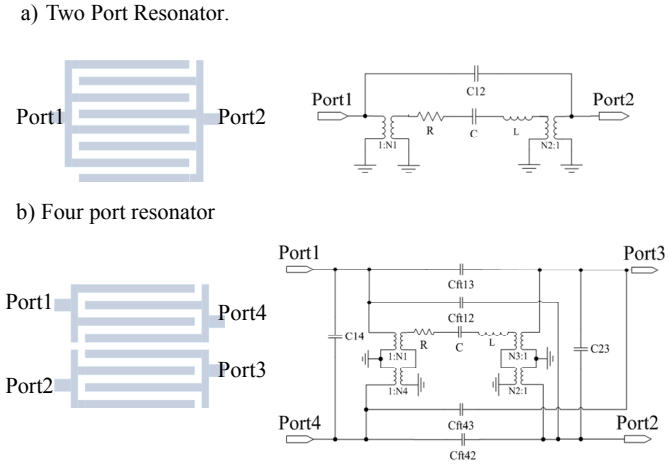

Figure 3. a) Two port resonator and simplified model. b) Four port resonator and simplified model.

Another important advantage of this topology is that shunt capacitance can be resonated out by using matching networks implemented with low Q (~ 20) on chip inductors. Hence insertion loss due to these capacitors can be removed. Alternatively, feed through capacitance is difficult to remove using inductances.

B. Resonator Scaling and Parasitics

Both two port and four port devices can be scaled in size to reduce the resonator impedance. Typically, the process used to release the device limits its size in one direction (width or length). For instance, in our work the width, W_d, of the device is limited to approximately 60 μm since our present release process allows for ~ 30 μm of undercut. Assuming we use the maximum width possible we can scale the length, L_e, to achieve further reductions in resonator motional impedance. However, this is not an ideal situation for scaling because of finger resistance and finger-to-finger capacitance. For frequencies below 12 GHz the fingers can be modeled as lumped RC. Ansoft's HFSS™ was used to determine the finger-to-finger capacitance for the 4.1 GHz device. It was found to be ~ 0.094 fF/μm. The resistance of the fingers is ~ 0.5 ohm per square. Simulation showed that loss in drive/sense signal due to the finger-to-finger capacitance was on the on the order of -0.1 dB confirming that a lumped or pi model can be used. Also this indicated that the finger resistance will limit IL even if the shunt (finger-to-finger) capacitance were removed through use of a matching network. Hence finger resistance, R_f, limits how long the device can be made. A simple case can be made for understanding how R_f causes loss in the resonator. Consider the current flow from port 1 through one finger, to port 3 (Figure 4). Note the series resistance from port 1 to ports 3,4 is always R_f no matter what position, x, at which the current leaves the finger and travels through the unit resonator to ports 3,4. Also it can be seen the worst case resistance is ~ 2 R_f from port 1 to 2 and ports 4 to 3.

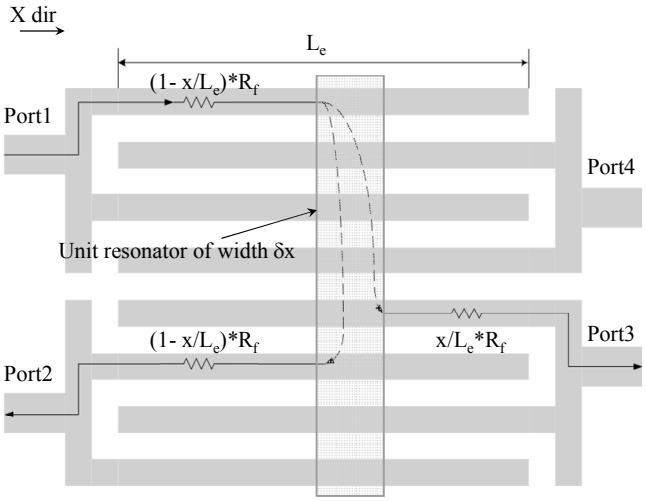

Figure 4. Current flow through the resonator. The dashed line indicates current flow through the AlN.

We can define a sub resonator or nanoresonator as done in [1]. The resistance of a single sub resonator, Rm, is given by (1), where ρ is the sub resonator resistivity per unit length. The total resistance, R_t, from one sub resonator to an adjacent one is equal to $R_m + R_f$. The minimum value for R_t can be shown to occur when L_e is equal to the optimum finger length L_{eopt}, (3). Thus, this simple analysis can be used to predict the optimum finger length in terms of effective material speed, c_{eff}, and desired frequency of operation, f_o (3). Note that κ is the sheet resistance of the top metal in ohms per square and $W_e = \lambda/4$, is the finger electrode width. Values for ρ and κ extracted from our process are: ρ = 72.54 kΩ·μm and κ = 0.5 ohms per square. This predicts an optimum length, $L_{eopt} \approx 300$ μm for the 4.1 GHz device which has $W_e = 630$ nm.

$$R_m \propto \frac{\rho}{L_e} \tag{1}$$

$$R_f \propto \kappa \frac{L_e}{W_e} \tag{2}$$

$$L_{eopt} \propto \sqrt{\frac{W_e \rho}{\kappa}} = \sqrt{\frac{c_{eff} \rho}{4 f_o \kappa}} \tag{3}$$

IV. Results of Scaling and Anchor Study

Width extensional devices with a center frequency of 4.1 GHz were fabricated varying L_e form 200 μm to 500 μm to investigate how insertion loss changes. Multiple die on the wafer were measured and the 300 μm device had the lowest IL which closely agrees with the analysis of the previous section. Figure 5 shows a measurement from one of the die. Clearly additional reductions in IL cannot be obtained by simply scaling the size of these devices because finger resistance will dominate as L_e is increased.

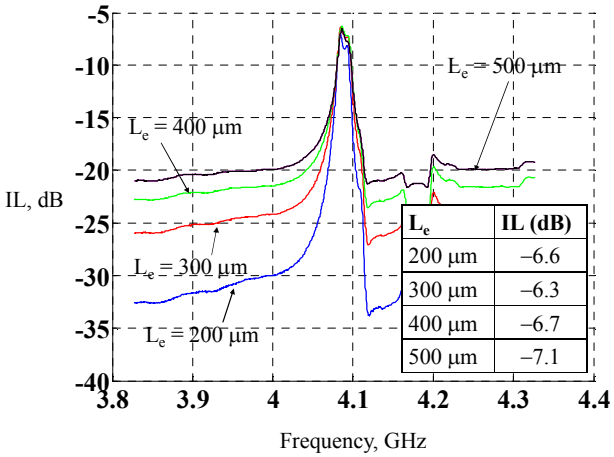

Figure 5. Insertion loss of 4.1 GHz device versus L_e. This was measured with an Agilent® E5071C Network analyzer using SOLT calibration. The differential transfer function is calculated with IL = 20 log(0.5*|(s31-s34)-(s21-s24)|). Note sij refers to the s parameters from port i to j.

A comparison was also performed between solidly anchored and beam anchored devices shown in Figure 1a,b. The best performing beam anchored resonators insertion loss were 2 dB worse than the best performing solidly anchored resonators. This is most likely due to the beam anchored resonators' narrow metal routing (Figure 1b), which adds about 60 ohms from device input to output. In addition, the Q's of the beam anchored resonators were comparable to the solidly anchored ones. On average the solidly anchored devices had better performance and much better yield when compared to the beam anchored device.

One unanticipated effect caused by using a four port topology was the dual peaking seen in the resonator transfer function (Figure 5). This phenomenon was first described in [4] where multiple resonances could be generated close to the fundamental mode by driving and sensing with separated electrodes. In [4] it was also reported that by changing the distance or overhang (Figure 6) from the resonator edge to the outermost electrodes these resonances could be moved. For our 4.1 GHz resonator this effect is clearly seen. A circuit model was developed using a transmission line model based on the work in [5]. The model is a one dimensional model (y dir as defined in Figure 1a) that breaks the device into sub resonators (Figure 6), one per electrode. Each sub resonator is modeled with a transmission line model adapted from [5]. Figure 6 compares the model to the measured data for a 4.1 GHz device. In order to get the model to match the overhang and transmission line loss (Q) were varied. A good match was obtained for a narrow bandwidth. However, the model did not match well over a wide range. This may be due to the fact that the model does not capture changes in damping over frequency. Hence, modes in the model may have more or less damping than in the actual physical case. In addition the model is only one dimensional and hence does not capture modes that can exist in multiple or other dimensions (x and z direction).

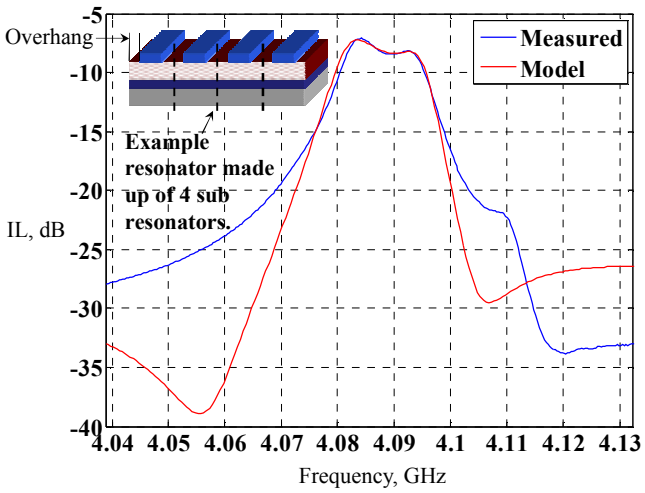

Figure 6. Comparsion of transmission line model to measured data.

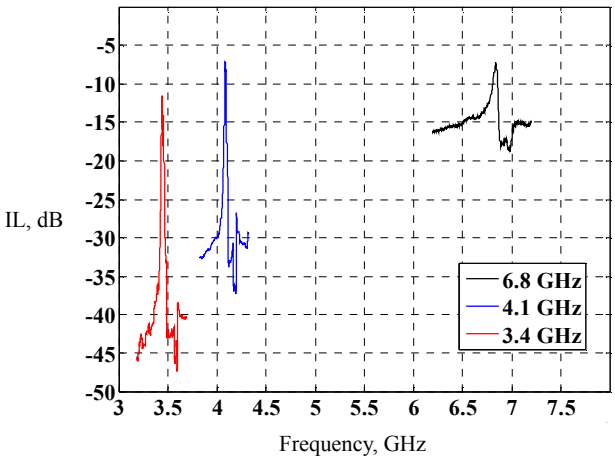

Figure 7. Plot of the SHF frequency responses using solidly anchored four port devices. Note the 6.8 GHz device has an insertion loss of -7.2 dB.

V. CONCLUSIONS

In this paper we demonstrate solidly anchored width extensional resonators at super high frequency that have been fabricated using fine line CMOS optical lithography tools. These resonators have achieved insertion losses as low as -6.4 dB at 4.1 GHz and -7.2 dB at 6.8 GHz (Figure 7). These are the lowest insertion loss SHF AlN devices reported to date. The four port topology decreases the feed through capacitance by an order of magnitude at 4 GHz when compared to two port topologies, thereby improving the stop band rejection of resonators and filters using this differential configuration. It has been shown that the solidly anchored devices have several advantages over their beam anchored counter parts. Metal used for signal routing from the resonator to the pad can be much wider than with beam anchored devices. Much larger separation of metal routes can also be employed. Thus reducing both parasitic resistance and feed through capacitance. Finally, there is no degradation in device IL or Q using the solidly anchored devices when compared to beam mounted devices. In fact we have shown that the solidly anchored resonators perform better than beam anchored devices at 500 MHz [3], when compared to the solidly anchored 500MHz device in [6], and at 4.1 GHz.

We have investigated the effects of parasitic finger resistance on scaling. Finger resistance is one of the main limiters in device scaling since it sets a maximum length above which IL start to increase. Therefore, further scaling to sub 50 ohms may require investigating process changes that include the ability to release devices larger devices. In our case we would want to increase the device width, W_d. The use of lower resistivity metals for metal routing both on top of the resonator and from the pads to the resonator should also be considered. It should be noted that increasing metal thickness on top of the resonator is not desirable as it will reduce material speed. One other alternative to scaling individual device size would be to place multiple devices in parallel. Device matching becomes an issue in this case.

Finally the four port configuration used to transduce the resonators inadvertently resulted in a filter response instead of a single resonance. This phenomenon has been explained in [4]. A model was developed which matches device behavior around the fundamental mode. In the future it may be possible to use this to implement SHF filters using the model to predict the filter response.

ACKNOWLEDGMENT

The authors would like to acknowledge the staff of the Microelectronics Develop Laboratory at Sandia National Laboratories for fabrication of the devices and Chris Nordquist and Mark Balance for use of their RF characterization resources.

REFERENCES

[1] M. Rinaldi, C. Zuniga, and G. Piazza, "5-10 GHz Contour-Mode Nanoelectromechanical Resonators, " *Micro Electro Mechanical Systems, 2009. 22th IEEE International Conference on MEMS* , pp. 916-919, Jan. 2009.

[2] M. Rinaldi, C. Zuniga, C. Zuo and G. Piazza, "Ultra-Thin Super High Frequency Two-Port ALN Contour-Mode Resonators and Filters," *IEEE International Solid-State Sensors, Actuators and Microsystems Conference*, pp. 577-580, June, 2009.

[3] R. H. Olsson III, C. M. Washburn, J. E. Stevens, M. R. Tuck, C. D. Nordquist, "VHF and UHF mechanically coupled aluminum nitride MEMS filters," *2008 IEEE International Frequency Control Symposium*, pp. 634-639, May 2008.

[4] C. R Perez, G. Piazza, "Bandwidth control in acoustically coupled AlN contour mode MEMS filters," *Frequency Control Symposium, 2009 Joint with the 22nd European Frequency and Time forum. IEEE International* , pp.64-69, April 2009.

[5] W. M. Leach, Jr., "Controlled-source analogous circuits and SPICE models for piezoelectric transducers," *IEEE Transactions on Ultrasonics, Ferroelectrics and Frequency Control*, vol.41, no.1, pp.60-66, Jan 1994.

[6] R. H. Olsson III, K. E. Wojciechowski, M. R. Tuck and J. E. Stevens, "Microresonant Impedance Transformers", *IEEE Ultrasonics Symposium*, Sept. 2009, in press.